Contents lists available at ScienceDirect

Science of the Total Environment

Fine-scale movement response of juvenile brown trout to hydropeaking

Robert Naudascher [a,b,*,1], Robert M. Boes [b], Vicente Fernandez [a], Joël Wittmann [a],
Markus Holzner [a,c], Davide Vanzo [b,d], Luiz G.M. Silva [a], Roman Stocker [a]

[a] *Institute of Environmental Engineering, Department of Civil, Environmental and Geomatic Engineering, ETH Zurich, Laura-Hezner-Weg 7, Zurich 8093, Switzerland*
[b] *Laboratory of Hydraulics, Hydrology and Glaciology, Department of Civil, Environmental and Geomatic Engineering, ETH Zurich, Hönggerbergring 26, Zurich 8093, Switzerland*
[c] *Swiss Federal Institute of Forest, Snow and Landscape Research WSL, Birmensdorf 8903, Switzerland*
[d] *Karlsruhe Institute for Technology, Institute for Water and Environment, Kaiserstrasse 12, Karlsruhe 76131, Germany*

HIGHLIGHTS

- Trout parr respond to hydropeaking within mere minutes.
- To cope with high flows, they swiftly relocate laterally and reduce exploratory behavior.
- Increased down-ramping rates result in shorter response times and increased relocation speed.

GRAPHICAL ABSTRACT
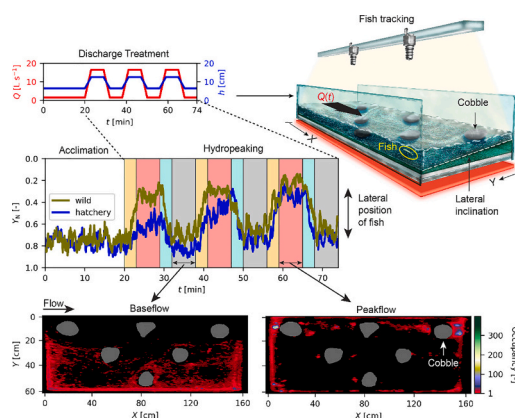
ARTICLE INFO

ABSTRACT

Juvenile fish are known to be the most impacted during hydropeaking events due to stranding or uncontrolled drift resulting from changes to water depth and flow velocity. To shed light on their response to such hydraulic alterations, we coupled flume experiments with image-based fish tracking and quantified the fine-scale movement behavior of wild ($n = 30$) and hatchery-reared ($n = 38$) brown trout (*Salmo trutta*) parr. We exposed fish to two distinct hydropeaking treatments in a laterally inclined (14 %) flume section stocked with real cobbles to create refuge and heterogeneous hydraulic conditions. Fish were individually acclimated (20 min) to baseflow ($Q = 1.6$ L s-1) and then exposed to three consecutive hydropeaking events, reaching peakflows tenfold larger than baseflow ($Q = 16$ L s-1). We found that, within just minutes, fish exhibited fine-scale movement responses to cope with the change of hydrodynamic conditions. Fish moved perpendicular to the main flow direction to shallow areas as these became submerged during discharge increase, holding position at low velocity zones. This

resulted in a significant difference ($p < 0.001$) in lateral occupancy of the experimental section between baseflow and peakflow. During peakflow, fish occupied specific positions around cobbles and exhibited swimming behaviors, including bow-riding and entraining, that allowed them to hold position while likely minimizing energy expenditure. As a result, swimming distance reduced 60–70 % compared to baseflow. During the decrease in discharge following peakflow, fish abandoned areas falling dry by moving laterally. In the treatment with the larger down-ramping rate, the time to initiate relocation was lower while the relocation speed was higher. This study shows that, for the conditions investigated here, brown trout parr is capable of swiftly deploying multiple behavioral responses to navigate rapid changes in hydrodynamic conditions. These findings can be incorporated into habitat modeling and improve our capacity to inform hydropeaking mitigation efforts.

1. Introduction

A key advantage of hydropower is its flexibility in energy production, as turbines may be started and stopped according to temporal fluctuations in electricity demand (Puffer et al., 2015). In this way, hydropower is able to buffer the intermittent supply of other renewable energy sources such as wind and solar (Dujardin et al., 2017; Braga, 2021), and thus play a key role in the energy transition away from fossil fuels. However, this operational flexibility results in rapid and often frequent changes in water discharge - known as hydropeaking - which cause unnatural fluctuations of flow conditions for riverine organisms: their ability to cope with these fluctuations is critical for their survival (Puffer et al., 2015).

Fish life history strategies have evolved in response to natural flow regimes (Bunn and Arthington, 2002), generally characterized by gradual discharge alterations over timescales of hours, days, seasons and years (Poff et al., 1997). In contrast, hydropeaking can induce rapid and unpredictable changes in discharge over timescales of just minutes (Young et al., 2011; Jones, 2014), which can cause dramatic changes in the location and availability of riverine habitats (Bätz et al., 2023) for fish and other organisms (Bipa et al., 2024). The adverse effects of hydropeaking on fish have been repeatedly reported (Schmutz et al., 2015; Auer et al., 2017; Hauer et al., 2017; Vanzo et al., 2023) and the importance of their mitigation has been recognized in regulatory frameworks (Federal Assembly of the Swiss Confederation, 2009; Tonolla, 2017). In fact, some European countries are currently implementing mitigation measures such as compensation basins (Reindl et al., 2023; Mchayk et al., 2024), while the cost efficiency of other measures, such as battery energy storage, is being investigated (Höfkes et al., 2024).

Fish can be affected at one or more stages of a hydropeaking event. As the discharge initially rapidly increases ("up-ramping phase"), fish can be displaced downstream ("forced drift") (Daufresne et al., 2005). This effect is more pronounced in larvae or juvenile fish that are less able to cope with the increase in flow velocities (Heggenes, 1988; Young et al., 2011). For example, the density and biomass of juvenile trout (*Salmo trutta*) were observed to be 30 % lower below hydropower dams as compared to upstream sites and this difference was largest in autumn, when the difference between natural and peakflow was greatest; in comparison, no significant difference was observed for adult fish (Lagarrigue et al., 2002). Significant forced drift during up-ramping was also observed for grayling (*Thymallus thymallus*) and nase (*Chondrostoma nasus*) in controlled experimental settings (Auer et al., 2017; Mameri et al., 2023).

When the discharge rapidly decreases again after peakflow ("down-ramping phase"), fish can be stranded on the dewatered substrate or become disconnected from the main channel in local depressions, resulting in injuries, desiccation and mortality (Saltveit et al., 2001; Young et al., 2011; Nagrodski et al., 2012; Harby and Noack, 2013). These effects are again more pronounced in the early life stages, such as larvae and fry. These life stages prefer habitats along the river shore, characterized by low mean flow velocities and low water depths (respectively 20–50 cm s^{-1} and < 20–30 cm for trout parr, Armstrong et al., 2003). These near-shore habitats are likely to shift in space during

the down-ramping phase (Bätz et al., 2023). Stranding of juvenile fish is considered to be the most severe effect of hydropeaking on fish populations (Young et al., 2011). For example, at river reaches with frequent hydropeaking, up to 59 % loss of salmon fry can occur within one season (Bauersfeld, 1978) and it has been argued that fish stranding can represent the main cause of fish community decline (Schmutz et al., 2015).

The rate of change of the discharge during hydropeaking ("ramping rate") has been identified as a crucial variable in predicting the severity of single hydropeaking events on fish (Schmutz et al., 2015; Bruder et al., 2016). The ramping rate directly determines how rapidly suitable habitats (hydraulically characterized in terms of water depth and flow velocity) are relocated during the course of a hydropeaking event (Shen and Diplas, 2010; Boavida et al., 2017). For example, stranding was found to increase with increasing down-ramping rates downstream of hydropower facilities (Hunter, 1992; Bradford and Cabana, 1997), in laboratory flumes (Halleraker et al., 2003) and in semi-natural outdoor flume facilities (Auer et al., 2017). The most likely explanation is that the time available for fish to relocate decreases as the ramping rate increases.

Although the ramping rate is an important parameter, stranding and drift are ultimately determined by the complex interaction between multiple behavioral (biotic) and physical (abiotic) factors. Among the latter, local depressions in the substrate and small values of the slope of the lateral banks are associated with increased stranding (Tuhtan et al., 2012; Auer et al., 2017; Boavida et al., 2017; Führer et al., 2022). In addition, river morphology plays a crucial role as it ultimately determines the total dewatered river bar width and the velocity at which the water-line recedes for a given ramping rate (Hayes et al., 2024). In contrast, drift decreases with the increasing availability of hydrodynamic shelter, provided for example by cobbles, and lateral flow refugia (Ribi et al., 2014; Costa et al., 2019a, b; Baladrón et al., 2021). Regarding biotic factors, life stage, species and reophilic response can affect drift rates (Zitek et al., 2004). For instance, during up-ramping in a small stream, juveniles (< 7 cm) of brown trout were more susceptible to downstream displacement than larger individuals (Heggenes and Traaen, 1988).

Most of our understanding of the effects of hydropeaking on fish is based on studies that quantified the number of drifted or stranded individuals under natural or laboratory conditions over large spatial scales (mesoscale or reach scale, i.e., meters to tens of meters). However, without the ability to track individual fish, understanding the behavioral responses driving these observations remains elusive. Ultimately, the large-scale distribution of a population result from the combined effects of the responses of individual organisms to environmental stimuli. Only recently have laboratory studies begun to investigate these behavioral responses under unsteady discharge conditions associated with hydropeaking for adult fish (Costa et al., 2018; Costa et al., 2019b). These approaches have relied on human observations of fish behavior, which are inherently limited in both spatial and temporal resolution. Similarly, field studies utilizing radio telemetry have demonstrated the impact of flow alterations on fish behavior (Boavida et al., 2017), yet with only 4–12 detections per day and a spatial resolution of 2 m, these studies are constrained to resolve broad behavioral patterns. Here we contribute to

address this gap by using video-based tracking of individual fish larvae subject to hydropeaking events in a laboratory setting, with high resolution in both space and time. This approach gives us access to detailed behavioral information, which can thus be connected to the spatial distribution patterns at the population level.

The fine-scale movement behavior of fish during unsteady flow conditions is poorly understood (Hayes et al., 2023). In particular, it is unclear whether early life stages of fish possess a suite of swimming behaviors that enable them to cope with rapid habitat shifts during periods of discharge alterations. To successfully cope with such alterations, fish would need to (i) recognize temporal changes of hydrodynamic conditions, to identify deterioration of local habitat, (ii) initiate relocation behavior, and (iii) relocate sufficiently rapidly to avoid stranding or downstream displacement. However, our understanding of when, whether and how individuals behaviorally respond to unsteady flow conditions remains elusive, particularly for juvenile fish.

This gap is particularly challenging to address as field or near-natural conditions make it difficult to track individuals from these early life-stages and the small body size prevents tagging, which would allow to determine their movement. Most rivers affected by hydropeaking in Europe and North America are inhabited by trout, which makes this a relevant target species to study hydropeaking effects on behavior (Hayes et al., 2019). Brown trout parr (*S. trutta*), hereafter referred to as trout, are territorial (Kalleberg, 1958; Fausch and White, 1981), preferring near-shore habitats with relatively low flow velocities (Fausch, 1984; Heggenes, 1988). It has been suggested that their reluctance to abandon their territory makes them especially vulnerable to the adverse effects of hydropeaking (Boavida et al., 2017). The aim of this study is to quantify the swimming behavior and spatial navigation of juvenile trout during hydropeaking conditions in a controlled flume setting that allows for highly time-resolved tracking of individual fish. We hypothesized that changes in flow discharge would significantly affect the spatial occupancy of fish, and we expected that hatchery-sourced and wild brown trout would exhibit different suites of behavioral responses. We further hypothesized that in treatments with a stronger ramping-rate, brown trout would display a faster lateral relocation response.

Our results have implications for understanding fundamental behavioral responses of juvenile fish in rapidly changing discharge conditions, with relevance for hydropeaking mitigation and conservation strategies.

2. Materials and methods

2.1. Experimental animals

A total of 40 hatchery (average standard length 5.9 ± 0.84 cm) and 44 wild trout (average standard length 5.8 ± 0.76 cm) were used for experimentation. Further details on fish origin are provided in Supplementary material, Text A.1 and Fig. S1. Experiments were performed using one fish at a time. After the experiments, wild fish were returned to their original sampling location, while hatchery fish were euthanized. Animal experimentation, handling procedures and husbandry were approved by the Zurich veterinary office (License no. 30997; Husbandry facility no. 182) and are described in Supplementary material, Text A.2 and Fig. S2.

2.2. Experimental procedures

Experiments were conducted from July 10 to August 14, 2020, during daytime (09:00 to 18:00) in an indoor hydraulic flume (length 25 m, width 0.6 m, longitudinal slope 0.5 %) at ETH Zurich (ETHZ), Switzerland (Supplementary material, Fig. S3). Using a recirculation system, water was continuously pumped into an upstream tank, from which it flowed into the open-channel flume and subsequently into a downstream tank. By regulating the pump rate we controlled the discharge in the flume. To ensure reproducible operation, key variables such as the flow rate in the water recirculation pipe (MID), the water level in the upstream and downstream tanks (Keller, Series $36\times$), the water level in the experimental section (NivuCont Plus) and the water temperature (Sensirion, SHT21) were continuously monitored. To implement hydropeaking treatments (TR1 and TR2) (Fig. 1 D,E), we used an automated Labview interface to regulate the pump rate (Supplementary material, Fig. S4). During experiments, the water temperature was maintained at $T = 12 \pm 0.5\,°C$ (identical to the husbandry tank) by a 20 kW cooling system (Clivet, KM Cool 20 CT), controlled by a thermostat. Flume water was replenished with tap water every three days and aeration stones were placed in the upstream tank to maintain dissolved oxygen concentrations of 7–10 mg L^{-1} (WTW CellOx 325, galvanic, membrane based).

To avoid possible effects of group size on behavior, and because trout parr are territorial (Kalleberg, 1958; Fausch and White, 1981), experiments were conducted with individual fish and each specimen was used only once. At the beginning of each experiment, a fish was captured in a bucket (4 L, avoiding direct air exposure) from the husbandry tank and placed within the bucked into the flume's experimental arena nearby. After 5 min acclimation within the bucket, the fish was released into the experimental arena (see next section) and kept there for another 5 min at baseflow conditions ($Q = 1.6$ L s^{-1}, Table 1). Thereafter, imaging was started, and the experimental arena was imaged for 20 min, constituting the acclimation phase (acclim), upon which the hydropeaking treatment begun. After completion of the treatment (62 min in TR1, 74 min in TR2), the fish was captured with the bucket and released in a dedicated compartment of the husbandry facility. Each run consisted of three steady baseflow periods (denoted by the letter "b") and three steady peakflows periods (denoted by the letter "p"), connected by periods of unsteady discharge conditions or "ramping phases" ("up" for up-ramping; "d" for down-ramping). In this manner, one experimental run consisted of a sequence of sub-phases, as follows: acclim, up1, p1, d1, b1, up2, p2, d2, b2, up3, p3, d3, b3.

2.3. Experimental arena

To allow for visual tracking of fish, a semi-transparent, laterally inclined (lateral slope = 14 %) gravel bed (Fig. 1 A,B) was fitted into a central section (length 1.6 m, width 0.6 m) of the flume (Supplementary material, Figs. S2A, S5). Its development was driven by three design criteria:

(1) create sufficient visual contrast for automated fish-tracking based on imaging fish from above through the water surface (Fig. 1C);

(2) avoid shining strong artificial light on fish so as not to impact their behavior; and

(3) mimic a heterogeneous gravel bed with a lateral gradient of water depth and flow velocity.

To avoid fish being disturbed by their own reflection at the glass walls, the latter were covered with perforated foil. To confine the experimental arena, honeycomb flow straighteners (diameter = 0.5 cm) were placed before the upstream and after the downstream ends of the arena. To increase the contrast between fish and background, we fabricated a translucent gravel bed by partly embedding glass gravel pebbles (length = 2–2.4 cm; diameter = 0.6–0.8 cm) into an epoxy layer. The arena was illuminated with infrared light (IR-light) from underneath the flume, using four LED strips emitting at wavelengths above 750 nm. The IR-light penetrated the glass bottom, a diffusor material, a color foil and the translucent gravel layer (Fig. 1A). A fish located in the arena appeared as a dark object in the image (Fig. 1C) as a result of preventing IR-light from reaching the camera. IR-light was used as the main light source since it is not visible for many fish species, including *Salmo trutta* (Bowmaker and Kunz, 1987), and has increasingly been used to observe fish behavior (Pautsina et al., 2015; Kerr et al., 2016; Lin et al., 2018). The color foil was fully translucent for infrared light ($\lambda > 750$ nm), yet absorbed light in the visible spectrum ($*\lambda = 400–700$ nm). Consequently, the gravel bed appeared dark for fish (and humans) in the
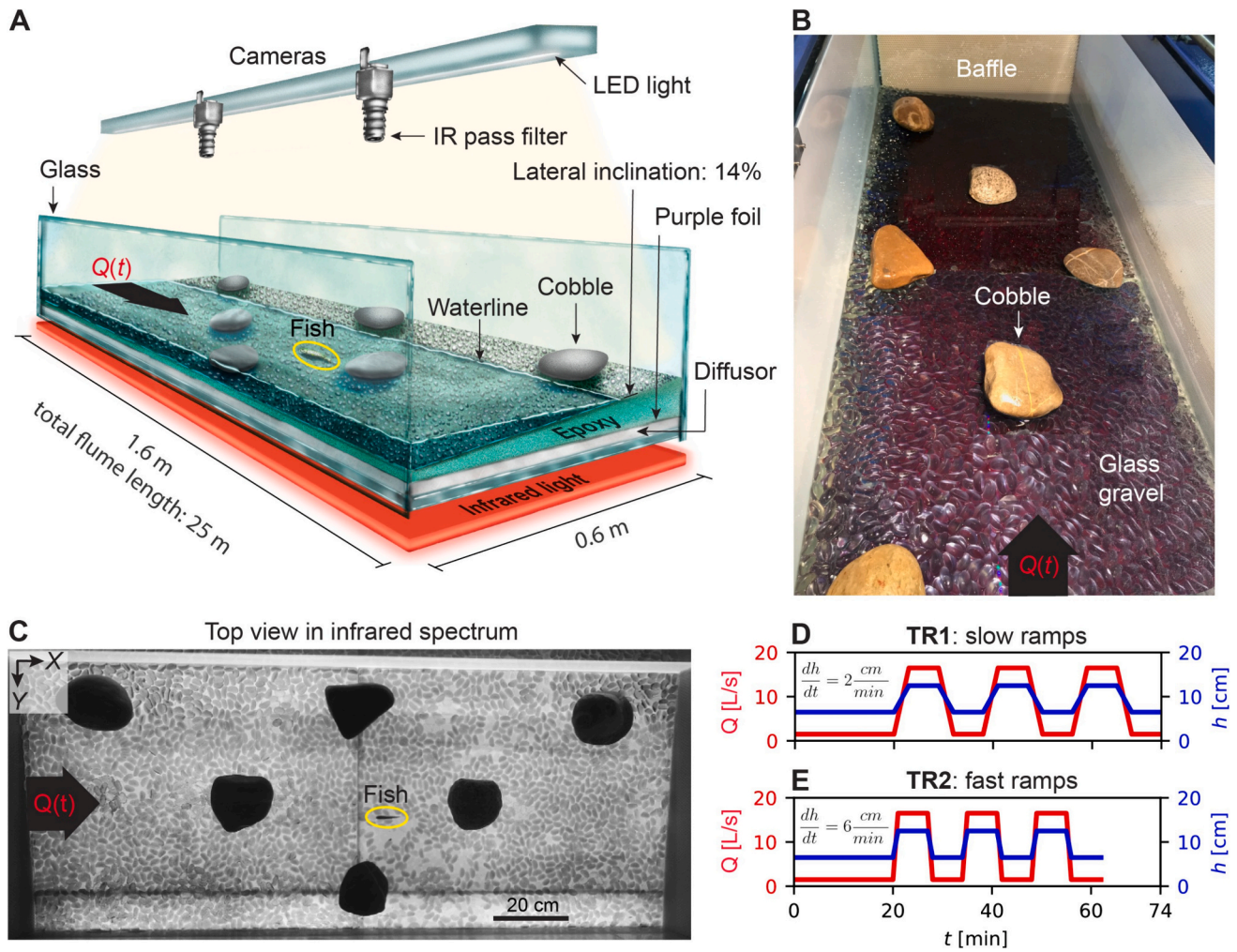
Fig. 1. The experimental arena and infrared- and visible-lighting setup. (A) Drawing of the experimental arena with translucent gravel bed and an individual fish, illustrated during baseflow conditions. Infrared light for homogeneous illumination originates from below the arena, penetrates through the glass bottom, a diffusive plastic plate, a purple foil and a laterally inclined epoxy gravel bed. Two cameras placed above the flume equipped with filters record only infrared light (760 nm $< \lambda$ < 860 nm). LED lights are used for mimicking daylight, emitting exclusively in the visual spectrum (400 nm $< \lambda < 720$ nm). Q indicates the discharge. (B) Photograph of the experimental arena consisting of a base layer of glass gravel pebbles (length $= 2$–2.4 cm; diameter $= 0.6$–0.8 cm) partly embedded in the epoxy base and six firmly attached natural cobbles (diameter ≈ 15 cm). (C) Top view of the experimental arena showing the glass gravel (light grey), the six cobbles (black) and a fish (highlighted by the yellow ellipse), which appears dark in the infrared spectrum. (D and E) Time series of the discharge Q (red) and of the water depth on the deep side of the gravel bed h (blue) for the two treatments TR1 (D) and TR2 (E). After a 20-min acclimation phase, during which the discharge remains constant at baseflow level, fish were exposed to three consecutive hydropeaking events characterized by peakflow and baseflow each lasting 6 min. The two treatments TR1 and TR2 differed only in the ramping rate dh/dt, given also in each panel's inset (TR1: 2 cm min^{-1}, TR2: 6 cm min^{-1}). For each treatment, the down-ramping rate is equal in magnitude and opposite in sign to the up-ramping rate.

Table 1
Hydraulic conditions in the experimental arena during baseflow and peakflow.

	Q	$h_{\min} - h_{\max}$	v_{bulk}	Submerged fraction
	[L s^{-1}]	[cm]	[cm s^{-1}]	[%]
Baseflow	1.6	0–6.5	8.1	66
Peakflow	16.5	4–12.5	35	100

visible spectrum (Fig. 1B), while at the same time providing a bright background for image-based fish tracking in the infrared spectrum (Fig. 1C). To imitate daylight, a single white-light LED strip (6500 K) was mounted at a height of 2.5 m above the flume. To eliminate light reflection at the water surface, cameras were provided with high-pass filters, preventing the visual light spectrum <750 nm from reaching the sensor.

2.4. Flow field

The time averaged two-dimensional flow field during baseflow and peakflow condition was obtained from Acoustic Doppler Velocimetry (ADV) measurements (Supplementary material, Fig. S6). The side-looking probes were placed along a spatial grid of dx = dy = 10 cm at a depth of z = 2 cm above the base-layer of the inclined epoxy inlet (Supplementary material, Fig. S5C). The instantaneous velocity components $u(t)$, $v(t)$, $w(t)$ were collected at a temporal resolution of 100 Hz and post-processed based on a standard procedure implemented in python (Agarwal et al., 2021).

The lateral inclination of the flume bed resulted in a lateral water-depth gradient of 14 % in the direction perpendicular to the main flow direction. Thus, during baseflow conditions ($Q_{\text{base}} = 1.6$ L s^{-1}; phases acclim, b1, b2 and b3), two thirds of the experimental arena was submerged, the averaged bulk flow velocity was $v_{\text{bulk}} = 8.1$ cm s^{-1}, and the water depth h varied laterally from 0 cm to 6.5 cm. During peakflow

conditions (phases p1, p2 and p3), the discharge was 10-fold higher ($Q_{peak} = 16.5$ L s^{-1}) the water depth was greater ($h = 4$–12.5 cm) and the entire experimental arena was submerged. During peakflow, the average bulk flow velocity increased more than four-fold, to $v_{bulk} = 35$ cm s^{-1} (Table 1).

To create a heterogeneous flow-field, six natural cobbles ($D \approx 15$ cm, height $= 4.8 \pm 0.6$ cm, Fig. 1B) were firmly glued to the base-layer of glass gravel. This ensured a reproducible flow field across experimental runs and a stationary background image (a basic requirement for automated tracking). Cobbles were distributed with increasing density toward the shallow side of the channel (Fig. 1A) to provide shelter and low-flow velocity zones (Supplementary material, Fig. S6A). Additionally, cobbles increased flow heterogeneity, in particular creating zones of lower flow velocities upstream and in their wake. During peakflow, all cobbles were fully submerged (Supplementary material, Fig. S5C), whereas during baseflow only the single cobble at the deepest location was fully submerged (Fig. 1B).

2.5. Experimental treatments

Experiments were performed using one fish at a time, therefore single individuals constitute a true replicate. We aimed to achieve meaningful statistical power while reducing the ethical burden of animal experimentation by using sample sizes consistent with previous behavioral studies in hydraulic flumes Boavida et al., 2017). The variation in sample size across treatments was caused by limited availability of wild-caught trout.

We defined two experimental treatments (TR1 and TR2) based on the ramping rate dh/dt that fish experienced during phases of flow transition (TR1: dh/d$t = 2$ cm min^{-1}; TR2: dh/d$t = 6$ cm min^{-1}). The two ramping rates were selected to study the impact of hydropeaking events of different severity on juvenile Brown trout, during daylight, guided by the Swiss hydropeaking mitigation guidelines (Tonolla, 2017). The range of water depth and bulk flow velocities during baseflow and peakflow were within the suitable habitat criteria of brown trout parr (Armstrong et al., 2003), mimicking local habitat conditions along the river shore.

An experimental run consisted of an acclimation phase at baseflow (20 min) followed by three consecutive and identical hydropeaking events, each consisting of up-ramping (3 min in TR1; 1 min in TR2), peakflow (p1, p2 and p3: 6 min each), down-ramping (3 min in TR1; 1 min in TR2) and baseflow (b1, b2 and b3: 6 min each) (Fig. 1D,E, Supplementary material, Fig. S4). All experiments were conducted with single fish (TR1 wild, $n = 16$; TR2 wild, $n = 14$; TR1 hatchery, $n = 20$; TR2 hatchery, $n = 18$).

2.6. Imaging and tracking of fish

Images were recorded using two temporally synchronized monochrome cameras (Mikrotron MC1318, 1280×1024 pixels) filming the experimental arena from above at 15 frames per second. With the cameras placed at a distance of 1.7 m from the arena, this yielded a resolution of 13.5 pixels/cm and a maximum refractive displacement error of $\Delta R_{max} = 0.9$ cm (Naudascher et al., 2024 *in preparation*). To prepare images for tracking, custom-made Python scripts were developed (openCV library; Bradski, 2000) and are available through a public GitHub repository (https://github.com/naroberto/hydropeaking). Thereby, the two camera views were merged into one image, rotated and cropped (python functions: cv2.FlannBasedMatcher, cv2.getRotationMatrix2D, cv2.warpPerspective). The goal of this pre-processing was to homogenize image size, orientation and origin of the coordinate system across experimental runs. As water absorbs infrared light, the water-level change during the ramping phase caused a substantial variation in illumination. Therefore, a moving background subtraction was applied to each image during the ramping phase, allowing to substantially reduce background noise and enhance visual contrast. To

obtain two-dimensional fish swimming trajectories, we used the animal tracking software "TRex" (Walter and Couzin, 2021) with previously optimized parameter sets for baseflow and peakflow conditions (Supplementary material, Table S1). The results of the automated tracking were manually reviewed for all videos and tracking errors corrected (Supplementary material, Text A.3). In total, we obtained trajectories for 70 individuals (TR1, 36 fish; TR2, 32 fish) during 58.8 h of video recordings.

2.7. Occupancy

To analyze preferred occupancy of different regions of the flow by fish during peakflow (p1, p2, p3) and baseflow conditions (b1, b2, b3), we generated 2D kernel density estimation (KDE) plots (python function: scipy.stats.gaussian_kde) based on the full trajectories ($X(t), Y(t)$) of all individual fish (Fig. 2A,B). By accounting for all individuals, these plots visualize occupancy hotspots at different times during treatment. Although fish occupancy may have been influenced by the downstream and upstream baffles or proximity to glass walls (i.e., thigmotaxis or wall-holding and tail-holding as described in Kerr et al., 2016), this effect was consistently present across all treatments and flow conditions. Therefore, we did not exclude these zones from our analysis. We normalized the occupancy values by dividing each value by the average occupancy across the entire arena (minus the area covered by cobbles), so that areas with values above one denote higher-than-average occupancy. We focus on these areas to determine preferred locations of fish.

2.8. Movement distance

The prevailing flow conditions significantly influenced the exploratory behavior of fish (Fig. 3A,C). To quantify this effect, we measured the movement distance R between consecutive points on trajectories of individual fish over timescales τ ranging from 0.2 to 55 s. This range of timescales approximately covers the range going from the temporal resolution of our imaging (15 fps) to the duration of the ramping periods (60 s).

2.9. Body posture

Fish body posture during peakflow and baseflow, quantified as the tail offset and the orientation angle, was directly obtained from the tracking code "TRex". The tail offset L ('midline_offset' in TRex) measures the offset of an individual's tail tip to the center line through its body, after aligning it with the x-axis such that its head is pointing against the flow. Positive and negative values of L indicate tail offsets in opposite directions. The orientation angle θ ('angle' in TRex) was measured so that $\theta = 0$ indicates alignment in the upstream direction, i. e. positive rheotaxis. Both posture quantities were derived from the fish body outline in each image and relied on the correct detection of fish head and tail. Due to distortions by surface waves, fish head and tail were at times swapped in the image analysis: these cases were identified by unnaturally high ($d\theta > 60°$) changes in orientation between consecutive frames (i.e. within 1/15 s), and discarded.

2.10. Statistical analysis

To compare the normalized lateral position between peakflow and baseflow (Fig. 2D,F), we performed the non-parametric Mann–Whitney *U* test (Supplementary material, Table S4). To test whether the observed increase in lateral relocation increased significantly over time, we conducted a Mann–Kendall test on peakflow phases (from p1 to p3) (Supplementary material, Table S5).
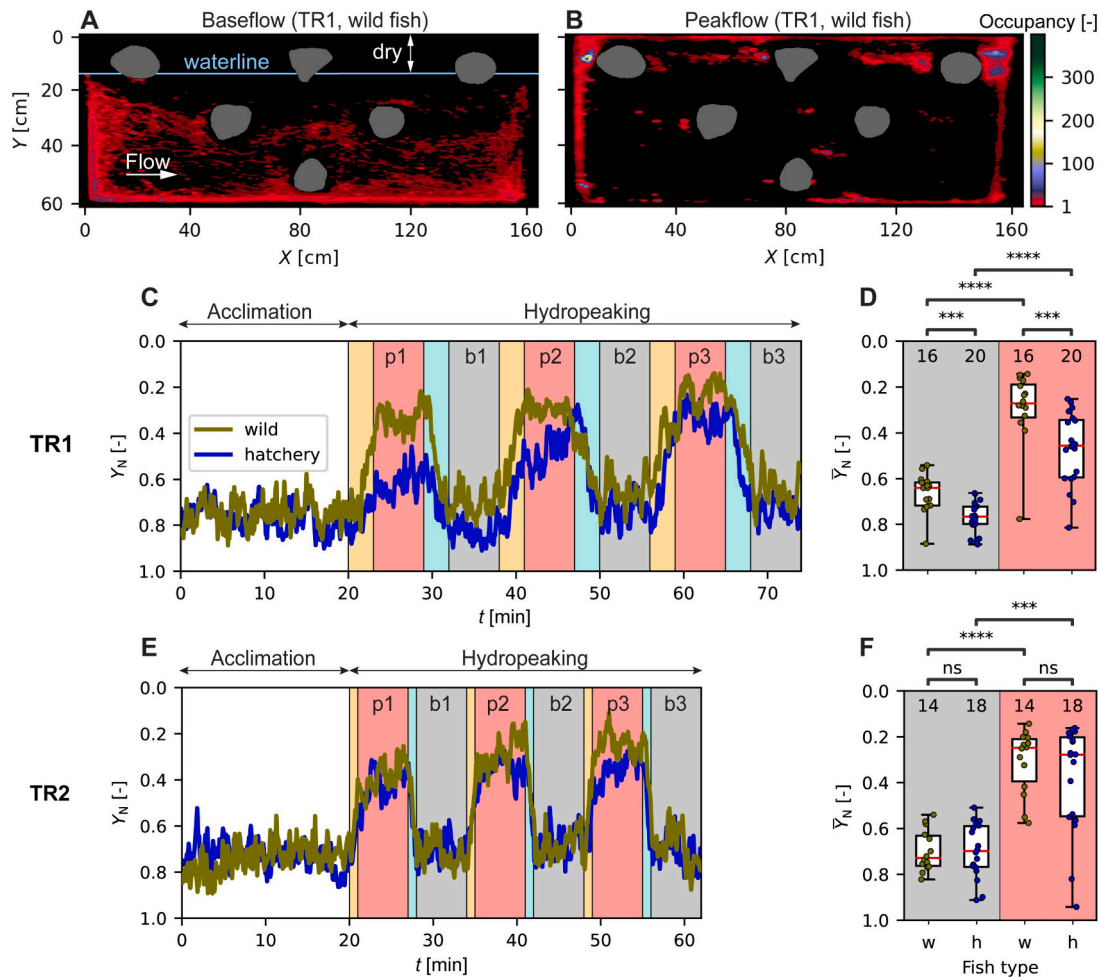
Fig. 2. Lateral relocation response of wild and hatchery fish in both treatments (TR1 and TR2). (A and B) Top view of the experimental arena showing a heatmap of wild fish trajectories ($n = 16$) during baseflow (A) and peakflow (B) in treatment TR1. A 2D Kernel density estimator (color gradient) was fitted to the normalized 2D-histogram of all locations of all fish, cumulated over (A) all three baseflow events (b1, b2 and b3) and (B) all three peakflow events (p1, p2 and p3). To indicate zones with above-average occupation, we divided each histogram value by the average occupancy across the domain and display only values >1 (see Methods). Flow is from left to right and cobbles are shown in grey. The coordinate system is defined in Fig. 1C. Note the presence of the waterline and a dry area during baseflow (panel A, $Y < 14$ cm). The entire experimental arena is submerged during peakflow (B). The same heatmaps for other conditions (TR1, hatchery fish; TR2, hatchery fish; TR2, wild fish) are shown in Supplementary material, Fig. S7 and S8. (C and E) Normalized lateral position Y_N of wild (green) and hatchery (blue) fish as a function of time during the acclimation period and the three hydropeaking events in treatments TR1 (C) and TR2 (E), respectively. The normalization of the lateral coordinate is based on the submerged width of the experimental arena, so that $Y_N = 0$ is the water-line on the shallow side at all times and $Y_N = 1$ is the deepest position. Background colors denote the different treatment phases (white = acclimation, orange = up-ramping, red = peakflow, grey = baseflow, turquoise = down-ramping). Note that the experimental duration of TR2 is shorter than TR1 because the ramping rate is higher (Fig. 1D,E) (D and F) Boxplots of the normalized lateral position $\overline{Y}_N$ averaged for all baseflow periods (b1, b2 and b3; grey background) and peakflow periods (p1, p2 and p3; red background) in treatments TR1 (D) and TR2 (F). The numbers above each plot indicate the number of fish imaged for that treatment. Whiskers show the full data range, circles represent individual fish, red lines indicate the median and the white box delimits the interquartile range. Results of statistical tests (Mann–Whitney U) are given above the plots (*** $p < 0.01$; **** $p < 0.001$; ns = not significant; see also Supplementary material, Table S4). Video animations of superimposed fish trajectories in TR1 and TR2 are shown in Supplementary material, A.4, Video V1, V2.

3. Results

3.1. Fish relocate laterally during hydropeaking

The locations within the experimental arena that fish occupied were strongly affected by the flow condition. During baseflow conditions (b1, b2, b3), fish predominantly occupied areas close to the upstream and downstream boundaries ($X = 0$–20 cm and $X = 140$–160 cm) and the deeper side of the arena ($Y = 50$–60 cm), with occupancies reaching levels up to 50-fold the average in a few regions (Fig. 2A). In contrast, during peakflow conditions (p1, p2, p3), fish displayed a strong preference (occupancies >100) for shallow-water areas ($Y = 0$–20 cm) (Fig. 2B), whereas most of the experimental arena was occupied below average (occupation density < 1, indicated in black). This strong

difference in occupancy between peakflow and baseflow was exhibited by both wild and hatchery fish and was observed in both hydropeaking treatments (TR1 and TR2) (Supplementary material, Fig. S7 and S8).

A temporal analysis of this relocation response revealed that the averaged lateral position of fish, Y_N (t) (Fig. 2C,E), was correlated with the discharge $Q(t)$ (Fig. 2D,E). During the up-ramping phase, fish moved toward the shallower part of the arena ($Y_N = 0.1$–0.4), preferentially remained there during peakflow (red background in Fig. 2C,E), then moved back to the deeper areas ($Y_N = 0.6$–0.8) during the down-ramping phase (turquoise background). This relocation toward and away from the shallow areas was repeatedly performed by wild and hatchery fish, in both treatments, and is clearly reflected by the differences in the normalized lateral position $\overline{Y}_N$ of fish during baseflow and peakflow conditions (Mann-Whitney-U test, $p < 10^{-3}$ for all significant
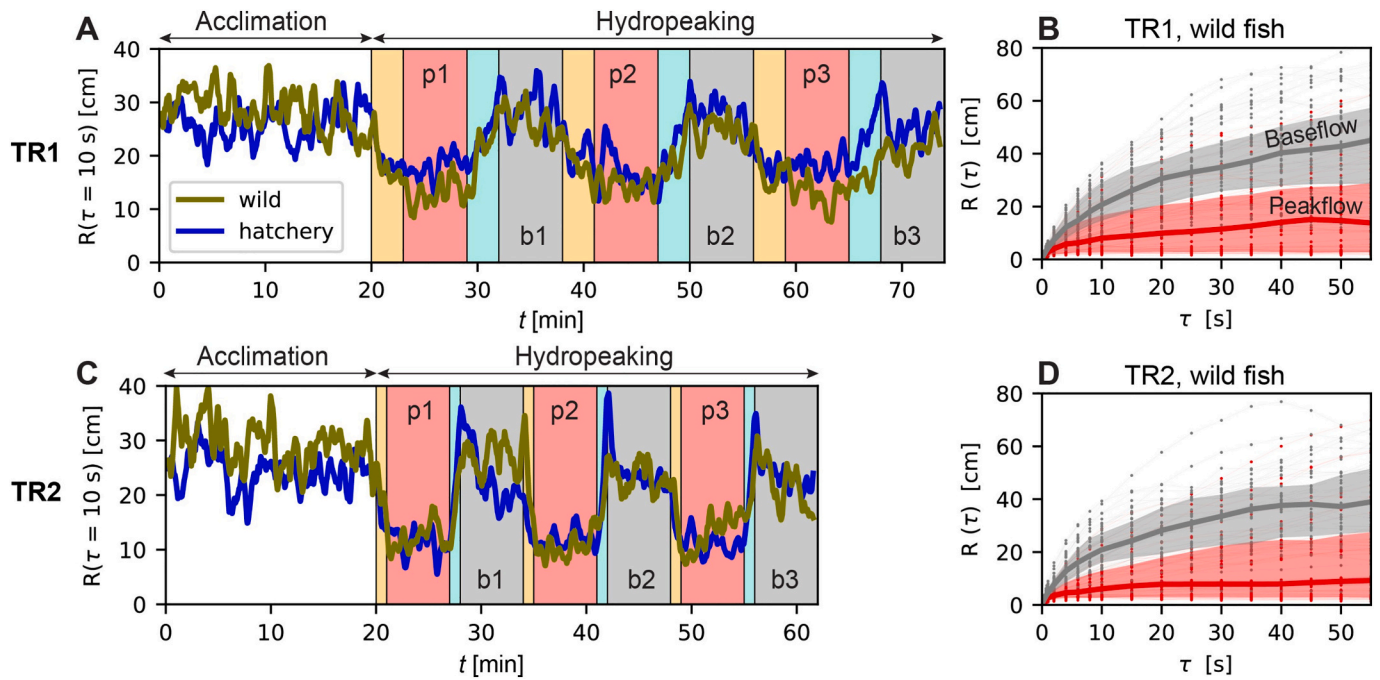
Fig. 3. Fish reduce exploratory behavior in peakflow conditions. (*A* and *C*). Fish movement distance $R(\tau) = \sqrt{\Delta x^2 + \Delta y^2}$ for a measurement timescale of $\tau = 10$ s for wild (green) and hatchery (blue) fish in treatments TR1 (*A*) and TR2 (*C*). The value of R was averaged across all individuals and smoothed in time using a moving average with a 30-s window. Background colors correspond to distinct hydropeaking phases (white = acclimation, orange = up-ramping, red = peakflow, grey = baseflow, turquoise = down-ramping). (*B* and *D*) The movement distance $R(\tau)$ (thick solid lines) of wild fish as a function of the measurement timescale τ, for $0.2\,\text{s} < \tau < 55\,\text{s}$, during baseflow (grey) and peakflow (red) for treatments TR1 (*B*) and TR2 (*D*). Points represent individual fish, thick solid lines are averages over all fish and shaded areas indicate the interquartile range (25th–75th percentiles). The corresponding plots for hatchery fish are shown in Supplementary material, Fig. S10.

differences, Fig. 2D,F. As a result of the higher density of cobbles and the lateral inclination of the bottom, both water depth and flow velocity decreased toward the shallower side of the arena ($Y < 20$ cm), (Supplementary material, Fig. S6). Thus, by retreating to the shallow water areas ($Y < 20$ cm) during peakflow, fish avoided exposure to higher flow velocities ($\sqrt{u^2 + v^2} > 0.4$ m s^{-1}), prevailing in the deeper and central part of the arena ($Y = 20$–50 cm) (Supplementary material, Fig. S6B).

In TR1 (slow ramping rate) the relocation response of wild fish was pronounced from the first hydropeaking event, whereas hatchery fish showed a weaker relocation response to the first event but then intensified their response over the ensuing two events (Fig. 2C) (Supplementary material, Fig. S9A). In TR2 (fast ramping rate) both wild and hatchery fish showed a pronounced response already to the first hydropeaking event. As a result, lateral occupancy of wild and hatchery fish differed significantly in TR1 (Mann-Whitney-*U* test, $p \langle 10^{-3}\rangle$ but not in TR2 (Fig. 2D,F). Both wild and hatchery fish in both treatments exhibited enhanced lateral relocation during the second and third hydropeaking peaks (p2 and p3) and this temporal trend was statistically significant (Mann-Kendall test, $p < 10^{-3}$, Table 2 and Supplementary material, Fig. S9C-F and Table S5).

3.2. Fish reduce exploratory behavior during peakflow

The average movement distance R of fish during peakflow was lower than during baseflow. For example, the average value of R (based on a timescale $\tau = 10$ s) of wild fish during peakflow (p1, p2 and p3) was 60–70 % lower ($R \approx 8$ cm in TR1 and $R \approx 6$ cm in TR2, i.e., 1–1.5 body lengths) than during baseflow (b1, b2 and b3; $R \approx 20$ cm in TR1 and TR2, i.e., 3.5 body lengths). This reduction in the movement distance, and thus in the exploratory behavior of fish, during peakflow was displayed by both wild and hatchery fish in both treatments (Fig. 3A,C). Further, this difference in the movement distance $R(\tau)$ was persistent across a broad range of timescales, $4 < \tau < 55$ s (Fig. 3B,D, Supplementary material, Figs. S10,S11). In particular, during peakflow, for timescales increasing above $\tau = 4$ s, R remained constant or in fact increased very mildly when compared to baseflow, reflecting the fact that during peakflow fish enter a behavioral mode of drastically reduced exploratory activity. This observation is supported by video animations of superimposed fish trajectories, which demonstrate that the majority of fish congregate at specific locations for extended periods of time, engaging solely in small-scale body motions over short timescales ($\tau < 4$ s) (Supplementary material, A.4, Video V1, V2).

3.3. Body posture reveals fine-scale behavior during peakflow

During peakflow, we observed that, in addition to relocating laterally (Fig. 2C,E), fish were drawn to particular zones in the immediate upstream and downstream of natural cobbles (Fig. 2B). Remarkably, these high-occupancy zones were the same for wild and hatchery fish in both treatments (Supplementary material, Fig. S8). We thus identified the dominant swimming modes within these zones. We quantified posture in terms of the orientation angle θ relative to the main flow direction and the tail tip offset L from the normalized central line (Fig. 4A,B). We distinguished distinct behavioral zones in the upstream and downstream

Table 2
Results of the Mann–Kendall test for the normalized lateral position Y_N during successive peakflows (p1, p2 and p3).

Treatment	Fish origin	Trend	*p*-Value	Intercept
TR1	Wild	Increasing	0.000001830	0.9
TR1	Hatchery	Increasing	0.000005400	0.92
TR2	Wild	Increasing	0.000415003	0.92
TR2	Hatchery	Increasing	0.000000098	0.85

of cobbles (Fig. 4C). Upstream of cobbles (during peakflow), fish displayed strong positive rheotaxis, with a narrow range of orientations ($-\pi/4 < \theta < \pi/4$) and small tail tip offsets (-0.3 cm $< L < 0.3$ cm), indicative of their body being aligned with the current and performing low amplitude tail beats (Fig. 4D), also visible in direct video observations (Supplementary material, A.4, Video V3). In contrast, downstream of cobbles (during peakflow) both the tail tip offset (-0.6 cm $< L < 0.6$ cm) and the orientation angle ($-\pi/2 < \theta < \pi/2$) had a broader distribution, with the orientation having a local minimum near $\theta = 0$ (Fig. 4E). This indicates that fish were more strongly tilted away from the flow direction and performed tail beats with larger amplitudes. Visual video analysis confirmed that downstream of cobbles fish engaged in repetitive swimming movements with large tail-beat amplitudes while being tilted away from the main flow direction ($\theta = 0$) (Supplementary material, A.4, Video V4). During baseflow, body posture patterns upstream and downstream of cobbles were very similar, characterized by a small range of tail tip offsets (-0.3 cm $< L < 0.3$ cm) and a wide range of orientation angles, indicative of a weaker interaction with the flow field (Fig. 4F,G). This trend was reproduced by wild fish in TR1 and hatchery fish in TR1 and TR2 (Supplementary material, Fig. S12).

3.4. Fish abandon shallow areas to avoid stranding

During peakflow a large fraction of fish occupied the shallower areas of the arena ($Y = 0$–20 cm; $h = 4$–6 cm). As these were the areas that fell dry during the ensuing down-ramping phase, fish had to abandon these areas to avoid being stranded. We identified 'shallow-water fish' (wild:

81 % in TR1 and TR2; hatchery: 47 % in TR1 and 60 % in TR2) as those whose average distance from the shore was smaller than a given threshold ($\bar{y} < 20$ cm) in the two minutes of peakflow preceding the down-ramping phase. We then analyzed the trajectories of these fish during the subsequent down-ramping phase (Fig. 5A,B and Supplementary material, S13). We found that, instead of swimming along a direct path toward areas of greater water depth, these fish exhibited tortuous relocation trajectories (Fig. 5A,B). The movement distance R(τ) strongly increased during down-ramping compared to peakflow, indicating an increase in exploratory behavior in response to the reduction in discharge (Fig. 3A,C). Indeed, R(τ) reached similar values to those observed during the acclimation period. However for hatchery fish in TR1 and TR2, R(τ) appeared to reach local maxima toward the end of the up-ramping phase. All fish in all treatments avoided stranding. Averaged over all 'shallow-water individuals', fish relocated from an average lateral position of $Y \approx 15$ cm during the last minute of peakflow to $Y \approx 50$ cm during the first minute of baseflow (Fig. 5C,D). However, this relocation response did not initiate immediately at the start of the down-ramping phase (at $t = 1$ min in Fig. 5C,D), but after some time ($\Delta t_R \approx 1$ min in TR1 and $\Delta t_R \approx 20$ s in TR2), reflecting a delayed response. Further, we found that during the central period of the down-ramping phase (TR1, 2 min $< t < 3$ min; TR2, 1.33 min $< t < 1.66$ min), fish changed lateral occupancy to move to the deeper side of the arena with an average lateral speed of $v_L = 14$ cm min^{-1} in TR1 and $v_L = 42$ cm min^{-1} in TR2 (Fig. 5C,D). Thus, both the relocation speed v_L and the relocation delay Δt were directly proportional to the down-ramping rate: the three-fold higher down-ramping rate in TR2 resulted in a three-fold increase in both v_L and Δt, as compared to TR1. Our results
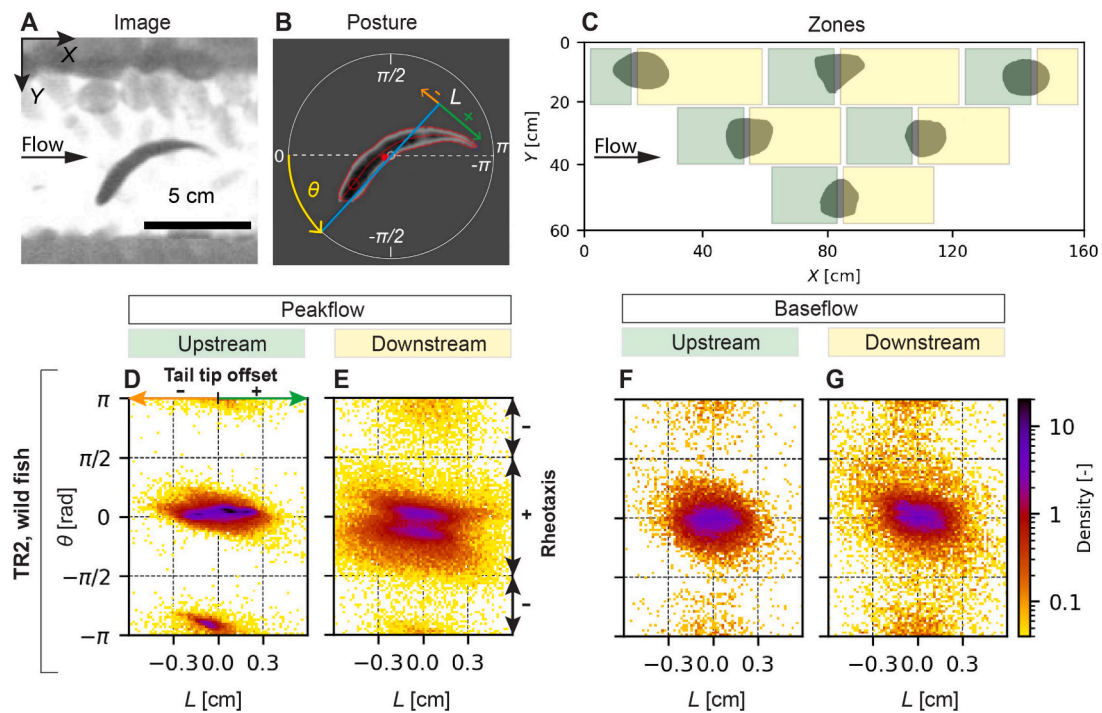

Fig. 4. Fish posture varies with position in the flow. (*A*) Grayscale infrared image of a fish during peakflow (only a small region of the full image is shown). (*B*) Variables used to characterize fish posture. The orientation angle θ is defined relative to the main flow direction X, so that positive rheotaxis (i.e., fish facing the current) results in $-\pi/2 < \theta < \pi/2$. The tail-tip offset L is defined as the distance of the tail tip to the body centerline (blue; see Methods, positive and negative values of L indicate tail offsets in opposite directions). Also shown is the body outline (red line), the center of gravity of the fish (red dot), and its head (red circle). (*C*) Fish posture was analyzed in distinct regions of the flow upstream of cobbles (green rectangles) and downstream of cobbles (yellow rectangles). (*D – G*) Two-dimensional probability density (see colorbar) of body posture quantified in terms of θ and L (see panel *B*), shown separately for different flow regions and conditions, for wild fish during TR2. All body postures of wild fish in TR2 during peakflow (p1, p2 and p3: *D* and *E*) and baseflow (b1, b2 and b3: *F* and *G*) upstream (*D* and *F*) and downstream of cobbles (*E* and *G*) are shown. Note that during baseflow, fish were never located within the uppermost regions of the flow ($Y < 20$ cm). The range $-\pi/2 > \theta > \pi/2$ denotes negative rheotaxis, while $-\pi/2 < \theta < \pi/2$ denotes positive rheotaxis. The corresponding plots for wild fish in TR1 and hatchery fish in TR1 and TR2 can be found in Supplementary material, Fig. S12. Video animations of fish posture during peakflow, analogous to *D* and *E* can be found in Supplementary material, Text A.4 and Videos V3, V4.
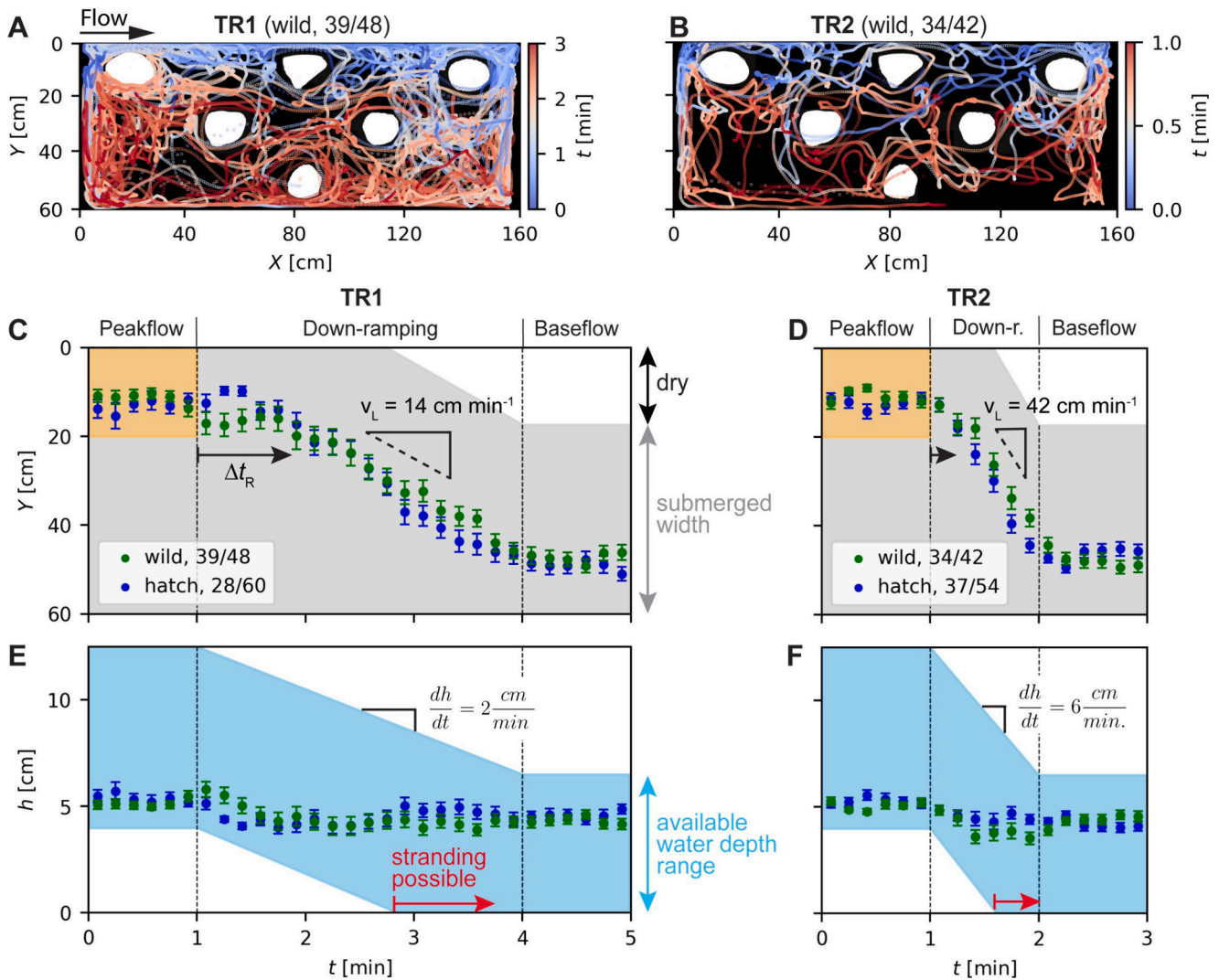
Fig. 5. Relocation of fish from shallow water during down-ramping phases ensuing p1, p2 and p3. Each fish was exposed to three down-ramping events per treatment (TR1 wild: $16 \times 3 = 48$ events; TR1 hatchery: $20 \times 3 = 60$ events; TR2 wild: $14 \times 3 = 42$ events; TR2 hatchery: $18 \times 3 = 54$ events). "Shallow-water fish" in TR1 (wild: 39; hatchery: 28) and TR2 (wild: 34; hatchery: 37) were defined as individuals with an average lateral position of $\bar{y} < 20$ cm during the 2 min preceding the start of the down-ramping phase. (A and B) Relocation trajectories of wild fish (X: streamwise position; Y: lateral position) during slow (A; TR1) and fast (B; TR2) down-ramping. Flow is from left to right and the color-coding (from blue to red) represents increasing time t. (C and D) Lateral relocation response of shallow-water fish in TR1 Time-series of the lateral position $Y(t)$ were averaged over time windows of 10 s. Points indicate the average lateral position of wild (green) and hatchery (blue) fish and error bars indicate the standard error of the mean. The orange area indicates the zone ($Y < 20$ cm) used to define shallow-water fish and the grey area shows the submerged width of the experimental arena. Triangles indicate the lateral relocation speed v_L and black arrows indicate the response time Δt_R. (E and F) Water-depth occupancy of shallow-water fish in TR1 (E) and TR2 (F). Points indicate the average local water depth occupied by wild (green) and hatchery (blue) fish, and error bars indicate the standard error of the mean. The available range of water depths is indicated in blue.

further indicate that by relocating laterally, shallow-water fish not only avoid being stranded, but also were able to continue to occupy a relatively narrow range of water depths (4 cm $< h <$ 6 cm) (Fig. 5E,F). Indeed, fish moved from the lower range of the available water depth at peakflow to the upper range of the available depth at baseflow, so that their water-depth occupancy changed relatively little in response to down-ramping. These observations were equally valid for wild and hatchery fish.

4. Discussion

In this study, we quantified the movement behavior of wild and hatchery trout parr during consecutive hydropeaking events on a confined, laterally inclined gravel slope. Fish relocated laterally and swiftly adapted their exploratory behavior in direct response to the changing discharge conditions.

4.1. Swimming activity and behavior during baseflow and peakflow

Our results demonstrate that trout parr movement activity was strongly influenced by the prevailing flow conditions. Fish exhibited significantly lower movement distances when flow velocities were high (20–40 cm s^{-1}; peakflow) compared to when they were low (0–20 cm s^{-1}; baseflow). Consistent with our findings, field observations of Arctic charr (*Salvelinus alpinus*, age 1+) in confined in-stream boxes (4 m^2) revealed that fish increased activity during low flow velocities (5.2 cm s^{-1}) but ceased activity almost completely during high flow velocities (21.1 cm s^{-1}) (Larranaga et al., 2018). Similarly, the exploratory behavior of trout and salmon (age class: 0+) was observed to increase during low flow in a natural stream (Riley et al., 2009) and a recent fine-scale telemetry study (grid $\approx$ 1 m) of juvenile Atlantic salmon found that increased discharge from hydropeaking reduced the likelihood of fish leaving their rearing habitat, decreasing both swimming distance and

variability in swimming direction during high flows (Matte et al., 2024 *in preparation*).

Salmonids employ a foraging strategy well-suited to life in flowing water: as 'drift feeders', they maintain an upstream-facing position (i.e. focal point) to capture prey delivered by the current (Piccolo et al., 2014). While the positioning in regions of high current velocities enhances prey encounter rates, it also raises the energetic cost of swimming (Everest and Chapman, 1972; Fausch, 1984; Hill and Grossman, 1993; Piccolo et al., 2014). Therefore, drift feeding salmonids maintain focal positions at relatively low water velocities, while foraging in the faster surrounding current (Jenkins, 1969; Everest and Chapman, 1972). Despite the absence of drifting food items in our study, we speculate that the trade-off between expected energy intake (i.e. prey encounter potential) and energy expenditure (swimming cost) could be the reason for the observed difference in exploratory behavior between peakflow and baseflow. During baseflow, increased mobility was favored by low swimming costs, prompting fish to increase movement distances (*R*), thereby enhancing potential prey encounters. Indeed, lower flow velocities have been shown to reduce both food availability (Nislow et al., 1998) and swimming costs (Hill and Grossman, 1993), which ultimately favours elevated mobility (Grant and Noakes, 1987). Conversely, during peakflow, high mobility was associated with high energetic costs for swimming, prompting fish to seek out hydrodynamically sheltered regions (see section 4.4) located in close proximity to high velocity regions, which allowed for potential foraging in the faster current. Supporting this interpretation, both observed (13 ± 8 cm s^{-1}) and predicted (12–21 cm s^{-1}) optimal focal point velocities for young trout (standard length ≈ 6.6 cm) in Coweeta Creek, USA (Hill and Grossman, 1993), were lower than most of the flow velocities present throughout our experimental arena during peakflow (Supplementary material, Fig. S6D,E).

4.2. Lateral relocation during up-ramping

During up-ramping phases, fish relocated laterally, reflecting an ability to respond to rapid up-ramping over short timescales, here on a scale of minutes (3 min in TR1, 1 min in TR2). Indeed, most fish relocated faster toward the shallow areas in TR2 than in TR1, suggesting that the relocation behavior was a direct response to the change in hydraulic conditions. Similarly, brown trout (SL ≥ 67 mm) in a small stream (Q = 350 L s^{-1}) were found to actively seek low-velocity niches within the gravel (Heggenes, 1988) during up-ramping phases lasting 15 min and it was separately argued that low-velocity microhabitats such as those found in coarse riverbeds can entirely prevent fish drift (Lobón-Cerviá, 1996).

4.3. Memory and temporal trends

The lateral relocation response became more pronounced over subsequent hydropeaking events, indicating that the ability of fish to respond to up-ramping improved over time. It is likely that fish were able to memorize the location of shallow water areas containing cobbles (located in the range $Y < 20$ cm) during previous peakflows and thus reached them more rapidly during later up-ramping phases. This hypothesis is supported by recent observations during multi-peaking experiments in a semi-natural outdoor channel. For similar peaking intervals (15 min) as used here, drift rates of young-of-the-year European grayling (*Thymallus thymallus*) and Nase (*Chondrostoma nasus*) declined after the first of multiple identical hydropeaking events, possibly due to the experience gained in reaching hydrodynamic shelter regions (Auer et al., 2023). Further, field studies with adult catfish (*Silurus glanis*) suggest that they can memorize past flow fluctuations for up to two weeks and avoid previously de-watered areas during hydropeaking (Capra et al., 2017). Indeed, several teleost fish species are able to memorize spatial characteristics of their habitats. The blind Mexican cave fish (*Astyanax fasciatus*) can learn and store hydrodynamic

information to build up a spatial map of its environment (De Perera, 2004) and the marine inter-tidal goby (*Bathygobius soporator*) can memorize the cm-scale reef bathymetry structure (Aronson, 1951; Aronson, 1971). Indeed, it was recently suggested that teleost fish species may possess a spatial encoding system (i.e. path integration) that parallels that of mammals, allowing them to return to previous locations along the most direct route even across unfamiliar terrain (Sibeaux et al., 2024).

Memory creation and retention may explain how fish accelerated their lateral relocation over ensuing peaks (p2 and p3) in our experiments. However, these observations are limited to the tested inter-peaking intervals of 18 and 14 min (TR1, TR2). Additionally, the confinement to a small, fixed bed might have favored the creation of spatial memory in comparison to a natural stream where confinement is absent or milder. Further research is needed to understand the existence and implications of memory over larger areas, dynamic gravel beds and longer inter-peaking intervals of hours or days.

4.4. Fish seek out hydrodynamic shelter during peakflows

During peakflow, fish (both wild and hatchery, and across both treatments) reduced exploratory behavior and displayed a strong preference for low-velocity zones on the shallow side of the arena ($v < 20$ cm s^{-1}; $Y \approx 0$–15 cm). Seeking lower flow velocities was likely a strategy to minimise the energetic cost associated with swimming (Webb, 1994). Similarly, fish have shown to shelter from high flow velocities during hydropeaking experiments by using lateral embayments (Almeida et al., 2017), flow deflectors (Costa et al., 2018), potholes (Auer et al., 2017), and in-stream structures (Costa et al., 2019b).

Different types of specialized swimming behaviors in turbulent flows have been characterized based on spatiotemporal patterns of body posture features (e.g., silhouette outline, orientation of the central line, tail-beat offset) obtained from imaging data (Liao, 2007). Here, we found distinctive patterns of body posture in the upstream and downstream of cobbles, which closely resemble previously described specialized swimming behaviors that are associated with a low energetic cost of swimming. These behaviors are bow riding and entraining (Supplementary material, A.4, Videos V3, V4).

Firstly, directly upstream of a cobble fish displayed a narrow range of body orientations in strong alignment with the main flow direction (i.e., θ close to 0) and small tail-beat offsets (i.e., small range of *L*), indicative of bow riding. These features are indeed characteristic of bow riding in the low-velocity, high-pressure zones upstream of bluff bodies (Liao, 2007). Bow riding has been observed for adult trout in front of cylinders (Liao et al., 2003) and dolphins in front of moving ships (Würsig, 2009).

Secondly, fish also preferentially occupied the area downstream of a cobble, where the lift and wake suction forces reduce hydrodynamic drag, in what is known as the entraining zone (Przybilla et al., 2010). Similar to entraining trout, which alternate between right and left sides in the downstream of a cylinder (Liao, 2006), our trout alternated between both downstream sides of a cobble, by tilting their body away from the main flow direction (i.e., $\theta \neq 0$) (Supplementary material, Text A.4, Video V4).

Characterized by repeated sequences of small-scale body motions, these behaviors contribute to explain the observed reduction in exploratory activity during peakflows (i.e., reduced movement distance *R*). These behaviors likely allowed fish to endure peakflow conditions at reduced energetic cost. For instance, previous experiments with rainbow trout (*Oncorhynchus mykiss*) revealed that entraining and bow waking demand up to 20 % less oxygen than free swimming (Taguchi and Liao, 2011).

These findings demonstrate the importance of energy conservation strategies for fish to cope with rapidly evolving, energetically demanding environments, highlighting the significance of available hydrodynamic shelters during hydropeaking (Puffer et al., 2015).

4.5. Movement response to down-ramping

Wild and hatchery fish successfully relocated laterally during the down-ramping phases in both treatments. Notably, the initiation of lateral relocation during the down-ramping phases exhibited a delay, with the delay being directly proportional to the rate of down-ramping. Thus, in TR1 the delay Δt_R was three times longer than in TR2, implying that in both treatments fish began to leave the shallower water at a similar value of the discharge ($Q \approx 10$ L s^{-1}). As water depth directly correlates with discharge, this suggests that in both treatments, fish on the shallow areas (e.g., $Y \approx 0\text{–}20$ cm) abandoned their initial holding positions when the local water-depth reached similar values ($h \approx 3\text{–}5$ cm). Although the changes in water velocity associated with the decrease of discharge may also have played a role in driving fish behavior, these results suggest that water depth was the primary hydraulic trigger causing fish to abandon shallow water areas.

The importance of water depth as a behavioral cue is also corroborated by a further observation. We found that the water depth occupancy remained relatively constant throughout the down-ramping phase in both treatments. Notably, the lateral relocation speed v_L increased proportionally to the down-ramping rate (which was 3-fold higher in TR2 than in TR1). Therefore, the faster temporal change of the available water depth range prompted fish to relocate more quickly. This direct relationship between the ramping rate and lateral relocation speed highlights the sensitivity of fish to changes in water depth during the down-ramping phase.

4.6. Behavioral difference of wild and hatchery fish

Wild and hatchery fish displayed consistent behaviors, including exploratory behavior and lateral relocation. This consistency suggests that these behaviors were not learned through experience (which hatchery fish do not possess) but are innate, i.e., genetically programmed. This general consistency notwithstanding, we observed some differences in the specifics of these behaviors. For example, hatchery fish displayed a weaker lateral relocation response than wild fish, indicating a reduced capacity to find and use hydrodynamic shelter during early up-ramping phases and peakflows (p1 and p2) in TR1, though interestingly not in TR2. Similarly, hatchery-reared brown trout in a natural stream displayed reduced utilization of cost-minimizing features in the substrate when compared to their wild conspecifics and it was postulated that high energy cost is a major cause of mortality among hatchery-reared brown trout stocked in streams (Bachman, 1984).

It is likely that wild fish were better accustomed to cope with discharge fluctuations than hatchery fish. Indeed, fish behavior and phenotype is strongly influenced by experiences and learning in their early-life environment (Huntingford, 2004; Gro Vea Salvanes and Braithwaite, 2006) and spatio-temporal complexity is a key feature of natural habitats (Braithwaite and Salvanes, 2005) that is lacking in artificial rearing environments (Johnsson et al., 2014). This deficit may help explain why hatchery fish displayed a weaker lateral relocation response in our study and complements previous observations of reduced behavioral flexibility and fitness of hatchery fish (Einum and Fleming, 2001; Salvanes et al., 2013).

4.7. Limitations

The behavioral observations in this study are in first instance specific to the bathymetric features (cobble size and layout, lateral inclination, glass gravel) and flow conditions, which ultimately dictated the fish's spatio-temporal flow-field experience. Indeed, lateral depth and velocity gradients possibly promoted lateral relocation behavior and cobbles provided hydrodynamic shelter during peakflows. However, we believe that the detailed behavioral information revealed by single-fish tracking may bear generality to other flow and substrate situations, and provides a blueprint for similar investigations in other environmental conditions.

Further research, both in the field and the laboratory, is needed to validate whether these findings are generalizable across other species, river bathymetries, ramping rates and hydropeaking frequencies. Therefore, we recommend caution in translating these results directly to inform hydropeaking mitigation measures.

5. Conclusion

This study sheds light on the dynamics of fish behavior during rapid flow alterations (i.e., timescales of minutes), thereby advancing our understanding of the ecological impacts of hydropeaking. Our results indicate that fish possess the ability to rapidly exhibit behavioral responses to changes in discharge (i.e. lateral relocation and a change in exploratory behavior), allowing them to cope with rapid flow fluctuations within just minutes. Overall, fish behavior during the up-ramping and peakflow phases appeared to be governed by energy-saving strategies, suggesting that natural river morphologies and coarse-gravel shorelines may provide hydrodynamic shelter for this life-stage. Ultimately, this raises important considerations with regard to river revitalisation projects in river stretches subject to hydropeaking: if similar refuge-seeking behavior toward lateral refuges is performed, downstream displacement (up-ramping phase) could be prevented, but the same refuges may trap fish during subsequent down-ramping phases. This underscores the necessity for further research to explore long-term effects, potential behavioral adaptations, and the influence of specific habitat features that provide hydrodynamic shelter.

Although we observed subtle differences in lateral occupancy between wild and hatchery fish in TR1, their behavioral response with respect to exploratory behavior, movement of shore fish and body posture did not differ significantly. This finding is relevant for the debate surrounding stocking practices and the appropriate source of fish for ethohydraulic experimentation both in the field and the laboratory.

We observed that fish are capable of enhancing their relocation response over the course of multiple hydropeaking events. This observation indicates that drift and stranding rates extrapolated from experiments with single hydropeaking events may overestimate the effects of hydropeaking when the latter occurs repeatedly over time, as is common in practice. However, it is still unclear to what extent reoccurring hydropeaking events may solely act as a selective pressure on recruitment or additionally prompt site specific adaptations (i.e. specific traits or behaviors) over evolutionary timescales. Similarly, our results have limited bearing on the role of the frequency of hydropeaking events, since a single frequency was tested.

Habitat models currently aim at predicting the distribution of organisms from a given species in space and time based on their measured or assumed preference for certain hydraulic conditions. Thereby, the results of a habitat model are coupled with species-specific and life-stage-specific habitat preferences. However, due to the limited understanding of the mechanisms that underpin the biophysical interactions between fish and their hydrodynamic environment, especially when it comes to temporal changes in flow conditions, habitat models currently fail to accurately predict the effects of the rapid relocation of preferred habitat resulting from hydropeaking. The findings of this study can contribute to allow habitat modellers to better incorporate behavioral aspects during periods of unsteady discharge conditions. For instance, hydraulic triggers for relocation and response times could be incorporated into existing models and enhance their ability to predict the risk of stranding in a given river reach. At the same time, further studies of this kind are needed to identify movement responses across environmental conditions, species, and life stages to make this modeling approach applicable outside the scenarios tested here.

Our results suggest that future research should investigate the long-term effects of hydropeaking on fish populations, considering the potential for sophisticated and rapidly deployed behavioral adaptations. The methods developed here may help to deepen our understanding of movement behavior in response to hydropeaking. Additionally,

understanding the specific habitat features that provide effective hydrodynamic shelter can inform river management and conservation strategies to mitigate the impacts of hydropeaking on aquatic ecosystems.

Supplementary data to this article can be found online at https://doi.org/10.1016/j.scitotenv.2024.175679.

CRediT authorship contribution statement

Robert Naudascher: Writing – original draft, Visualization, Validation, Software, Methodology, Investigation, Formal analysis, Data curation, Conceptualization. **Robert M. Boes:** Writing – review & editing, Supervision, Funding acquisition, Conceptualization. **Vicente Fernandez:** Supervision, Conceptualization. **Joël Wittmann:** Data curation. **Markus Holzner:** Writing – review & editing, Supervision. **Davide Vanzo:** Writing – review & editing, Conceptualization. **Luiz G. M. Silva:** Writing – review & editing, Supervision, Conceptualization. **Roman Stocker:** Writing – review & editing, Supervision, Funding acquisition, Conceptualization.

Declaration of competing interest

The authors declare that they have no known competing financial interests or personal relationships that could have appeared to influence the work reported in this paper.

Data availability

The Python scripts used for the image prepossessing are available through a public GitHub repository (https://github.com/naroberto/hydropeaking). The generated video animations can be accessed through an open access archive (doi:https://doi.org/10.3929/ethz-b-000679140).

References

Agarwal, M., Deshpande, V., Katoshevski, D., Kumar, B., 2021. A novel python module for statistical analysis of turbulence (p-SAT) in geophysical flows. Sci. Rep. 11 (1), 3998. https://doi.org/10.1038/s41598-021-83212-1.

Almeida, R., Boavida, I., Pinheiro, A., 2017. Habitat modeling to assess fish shelter design under hydropeaking conditions. Can. J. Civ. Eng. 44 (2), 90–98. https://doi.org/10.1139/cjce-2016-0186.

Armstrong, J.D., Kemp, P.S., Kennedy, G.J.A., Ladle, M., Milner, N.J., 2003. Habitat requirements of Atlantic salmon and brown trout in rivers and streams. Fish. Res. 62 (2), 143–170. https://doi.org/10.1016/S0165-7836(02)00160-1.

Aronson, L.R., 1951. Orientation and Jumping Behavior in the Gobiid Fish Bathygobius Soporator. American Museum Novitates; no. 1486. American Museum of Natural History, New York.

Aronson, L.R., 1971. Further studies on orientation and jumping behavior in the gobiid fish, bathygobius soporator. Ann. N. Y. Acad. Sci. 188 (1), 378–392. https://doi.org/10.1111/j.1749-6632.1971.tb13110.x.

Auer, Zeiringer, B., Führer, S., Tonolla, D., Schmutz, S., 2017. Effects of river bank heterogeneity and time of day on drift and stranding of juvenile european grayling (thymallus thymallus l.) caused by hydropeaking. Sci. Total Environ. 575, 1515–1521. https://doi.org/10.1016/j.scitotenv.2016.10.029.

Auer, Führer, Simon, Hayes, Daniel, Zeiringer, Bernhard, Schmutz, Stefan, 2023. The Influence of Repeated Hydropeaking Events on Early Live Stages of European Grayling (*thymallus thymallus*) and Common Nase (*chondrostoma nasus*).

Bachman, R.A., 1984. Foraging behavior of free-ranging wild and hatchery brown trout in a stream. Trans. Am. Fish. Soc. 113 (1), 1–32. https://doi.org/10.1577/1548-8659(1984)113<1:FBOFWA>2.0.CO;2.

Baladrón, A., Costa, M.J., Bejarano, M.D., Pinheiro, A., Boavida, I., 2021. Can vegetation provide shelter to cyprinid species under hydropeaking? Sci. Total Environ. 769, 145339 https://doi.org/10.1016/j.scitotenv.2021.145339.

Bätz, N., Judes, C., Weber, C., 2023. Nervous habitat patches: the effect of hydropeaking on habitat dynamics. River Res. Appl. 39 (3), 349–363. https://doi.org/10.1002/rra.4021.

Bauersfeld, K., 1978. Stranding of Juvenile Salmon by Flow Reductions at Mayfield Dam on the Cowlitz River, 1976. State of Washington, Department of Fisheries. https://books.google.ch/books?id=uDB4GQAACAAJ.

Bipa, N.J., Stradiotti, G., Righetti, M., Pisaturo, G.R., 2024. Impacts of hydropeaking: a systematic review. Sci. Total Environ. 912, 169251 https://doi.org/10.1016/j.scitotenv.2023.169251.

Boavida, I., Harby, A., Clarke, K.D., Heggenes, J., 2017. Move or stay: habitat use and movements by Atlantic salmon parr (salmo salar) during induced rapid flow variations. Hydrobiologia 785 (1), 261–275. https://doi.org/10.1007/s10750-016-2931-3.

Bowmaker, J., Kunz, Y., 1987. Ultraviolet receptors, tetrachromatic colour vision and retinal mosaics in the brown trout (salmo trutta): age-dependent changes. Vis. Res. 27 (12), 2101–2108. https://doi.org/10.1016/0042-6989(87)90124-6.

Bradford, M.J., Cabana, G., 1997. Interannual variability in stagespecific survival rates and the causes of recruitment variation. In: Chambers, R.C., Trippel, E.A. (Eds.), Early Life History and Recruitment in Fish Populations. Springer, Netherlands, pp. 469–493. https://doi.org/10.1007/978-94-009-1439-1_17.

Bradski, G., 2000. The openCV library. [ISBN: 1044-789X Publisher: Miller Freeman Inc.]. Dr. Dobb's Journal: Software Tools for the Professional Programmer 25 (11), 120–123.

Braga, D., 2021. Integration of energy storage systems into the power system for energy transition towards 100% renewable energy sources. In: 2021 10th International Conference on ENERGY and ENVIRONMENT (CIEM), pp. 1–5. https://doi.org/10.1109/CIEM52821.2021.9614778.

Braithwaite, V.A., Salvanes, A.G.V., 2005. Environmental variability in the early rearing environment generates behaviourally flexible cod: implications for rehabilitating wild populations. Proc. Biol. Sci. 272 (1568), 1107–1113. https://doi.org/10.1098/rspb.2005.3062.

Bruder, A., Tonolla, D., Schweizer, S.P., Vollenweider, S., Langhans, S.D., Wüest, A., 2016. A conceptual framework for hydropeaking mitigation. Sci. Total Environ. 568, 1204–1212. https://doi.org/10.1016/j.scitotenv.2016.05.032.

Bunn, S.E., Arthington, A.H., 2002. Basic principles and ecological consequences of altered flow regimes for aquatic biodiversity. Environ. Manag. 30 (4), 492–507. https://doi.org/10.1007/s00267-002-2737-0.

Capra, H., Plichard, L., Bergé, J., Pella, H., Ovidio, M., McNeil, E., Lamouroux, N., 2017. Fish habitat selection in a large hydropeaking river: strong individual and temporal variations revealed by telemetry. Sci. Total Environ. 578, 109–120. https://doi.org/10.1016/j.scitotenv.2016.10.155.

Costa, Boavida, I., Almeida, V., Cooke, S., Pinheiro, A., 2018. Do artificial velocity refuges mitigate the physiological and behavioural consequences of hydropeaking on a freshwater iberian cyprinid?: do refuges mitigate the consequences of hydropeaking on a cyprinid? Ecohydrology 11 (7), e1983. https://doi.org/10.1002/eco.1983.

Costa, Ferreira, M.T., Pinheiro, A.N., Boavida, I., 2019a. The potential of lateral refuges for iberian barbel under simulated hydropeaking conditions. Ecol. Eng. 127, 567–578. https://doi.org/10.1016/j.ecoleng.2018.07.029.

Costa, M.J., Fuentes-Pérez, J.F., Boavida, I., Tuhtan, J.A., Pinheiro, A.N., 2019b. Fish under pressure: examining behavioural responses of iberian barbel under simulated hydropeaking with instream structures (D. M. Higgs, Ed.). PLoS One 14 (1), e0211115. https://doi.org/10.1371/journal.pone.0211115.

Daufresne, M., Capra, H., Gaudin, P., 2005. Downstream displacement of post-emergent brown trout: effects of development stage and water velocity. J. Fish Biol. 67 (3), 599–614. https://doi.org/10.1111/j.0022-1112.2005.00759.x.

De Perera, T.B., 2004. Fish can encode order in their spatial map. Proc. R. Soc. Lond. Ser. B Biol. Sci. 271 (1553), 2131–2134. https://doi.org/10.1098/rspb.2004.2867.

Dujardin, J., Kahl, A., Kruyt, B., Bartlett, S., Lehning, M., 2017. Interplay between photovoltaic, wind energy and storage hydropower in a fully renewable Switzerland. Energy 135, 513–525. https://doi.org/10.1016/j.energy.2017.06.092.

Einum, S., Fleming, I.A., 2001. Implications of stocking: ecological interactions between wild and released salmonids [Publisher: BLOMS BOKTRYCKERI AB]. Nord. J. Freshw. Res. 75, 56–70.

Everest, F.H., Chapman, D.W., 1972. Habitat selection and spatial interaction by juvenile Chinook salmon and steelhead trout in two Idaho streams. J. Fish. Res. Board Can. 29 (1), 91–100. https://doi.org/10.1139/f72-012.

Fausch, K.D., 1984. Profitable stream positions for salmonids: relating specific growth rate to net energy gain. Can. J. Zool. 62 (3), 441–451. https://doi.org/10.1139/z84-067.

Fausch, K.D., White, R.J., 1981. Competition between brook trout (*Salvelinus fontinalis*) and brown trout (*Salmo trutta*) for positions in a Michigan stream. Can. J. Fish. Aquat. Sci. 38 (10), 1220–1227. https://doi.org/10.1139/f81-164.

Federal Assembly of the Swiss Confederation, 2009. Revision - bundesgesetz über den schutz der gewässer. Retrieved January 6, 2019, from. https://www.newsd.admin.ch/newsd/message/attachments/20578.pdf.

Führer, S., Hayes, D.S., Hasler, T., Graf, D.R.M., Fauchery, E., Mameri, D., Schmutz, S., Auer, S., 2022. Stranding of larval nase (chondrostoma nasus l.) depending on bank slope, downramping rate and daytime [Publisher: Frontiers]. Frontiers in Environmental Science 10. https://doi.org/10.3389/fenvs.2022.966418.

Grant, J.W.A., Noakes, D.L.G., 1987. A simple model of optimal territory size for drift-feeding fish [Publisher: NRC Research Press]. Can. J. Zool. 65 (2), 270–276. https://doi.org/10.1139/z87-042.

Gro Vea Salvanes, A., Braithwaite, V., 2006. The need to understand the behaviour of fish reared for mariculture or restocking. ICES J. Mar. Sci. 63 (2), 345–354. https://doi.org/10.1016/j.icesjms.2005.11.010.

Halleraker, J.H., Saltveit, S.J., Harby, A., Arnekleiv, J.V., Fjeldstad, H.-P., Kohler, B., 2003. Factors influencing stranding of wild juvenile brown trout (salmo trutta) during rapid and frequent flow decreases in an artificial stream. River Res. Appl. 19 (5), 589–603. https://doi.org/10.1002/rra.752.

Harby, A., Noack, M., 2013. Rapid flow fluctuations and impacts on fish and the aquatic ecosystem. In: Ecohydraulics. John Wiley & Sons, Ltd., pp. 323–335. https://doi.org/10.1002/9781118526576.ch19. Retrieved May 17, 2024, from.

Hauer, C., Siviglia, A., Zolezzi, G., 2017. Hydropeaking in regulated rivers – from process understanding to design of mitigation measures. Sci. Total Environ. 579, 22–26. https://doi.org/10.1016/j.scitotenv.2016.11.028.

Hayes, Moreira, M., Boavida, I., Haslauer, M., Unfer, G., Zeiringer, B., Greimel, F., Auer, S., Ferreira, T., Schmutz, S., 2019. Life stage-specific hydropeaking flow rules. Sustainability 11 (6), 1547. https://doi.org/10.3390/su11061547.

Hayes, Bruno, M., Alp, M., Boavida, I., Batalla, R., Bejarano, M., Noack, M., Vanzo, D., Casas-Mulet, R., Vericat, D., Carolli, M., Tonolla, D., Halleraker, J., Gosselin, M.-P., Chiogna, G., Zolezzi, G., Venus, T., 2023. 100 key questions to guide hydropeaking research and policy. Renew. Sust. Energ. Rev. 187, 113729 https://doi.org/10.1016/j.rser.2023.113729.

Hayes, Hauer, C., Unfer, G., 2024. Fish stranding in relation to river bar morphology and baseflow magnitude: combining field surveys and hydrodynamic–numerical modelling [_eprint: https://onlinelibrary.wiley.com/doi/pdf/10.1002/eco.2616]. Ecohydrology 17 (2), e2616. https://doi.org/10.1002/eco.2616.

Heggenes, J., 1988. Effects of short-termflowfluctuations on displacement of, and habitat use by, brown trout in a small stream [Publisher: Taylor & Francis _eprint: doi: 10.1577/1548-8659(1988)117<0336:EOSFFO>2.3.CO;2]. Trans. Am. Fish. Soc. 117 (4), 336–344. https://doi.org/10.1577/1548-8659(1988)117<0336:EOSFFO>2.3.CO;2.

Heggenes, J., Traaen, T., 1988. Downstream migration and critical water velocities in stream channels for fry of four salmonid species. J. Fish Biol. 32 (5), 717–727. https://doi.org/10.1111/j.1095-8649.1988.tb05412.x.

Hill, J., Grossman, G.D., 1993. An energetic model of microhabitat use for rainbow trout and rosyside dace. Ecology 74 (3), 685–698. https://doi.org/10.2307/1940796.

Höfkes, G.F., Evers, F.M., Hohermuth, B., Boes, R.M., 2024. Hybrid hydropeaking mitigation at storage hydropower plants combining compensation basins with battery energy storage systems (BESS). J. Energy Storage 86, 111247. https://doi.org/10.1016/j.est.2024.111247.

Hunter, 1992. Hydropower Flow Fluctuations and Salmonids: A Review of the Biological Effects, Mechanical Causes, and Options for Mitigation (State of Washington Department of Fisheries No. 119). State of Washington Department of Fisheries.

Huntingford, F.A., 2004. Implications of domestication and rearing conditions for the behaviour of cultivated fishes. J. Fish Biol. 65, 122–142. https://doi.org/10.1111/j.0022-1112.2004.00562.x.

Jenkins, T.M., 1969. Social structure, position choice and micro-distribution of two trout species (salmo trutta and salmo gairdneri) resident in mountain streams. Anim. Behav. Monogr. 2, 55–123. https://doi.org/10.1016/S0066-1856(69)80002-6.

Johnsson, J.I., Brockmark, S., Näslund, J., 2014. Environmental effects on behavioural development consequences for fitness of captivereared fishes in the wild. J. Fish Biol. 85 (6), 1946–1971. https://doi.org/10.1111/jfb.12547.

Jones, N.E., 2014. The dual nature of hydropeaking rivers: is ecopeaking possible? River Res. Appl. 30 (4), 521–526. https://doi.org/10.1002/rra.2653.

Kalleberg, H., 1958. Observations in a Stream Tank of Territoriality and Corn· Petition in Juvenile Salmon and Trout (*salmo salar* L. and s. Trutta L.), vol. No. 39. Institute of Freshwater Research, Drottningholm.

Kerr, J.R., Manes, C., Kemp, P.S., 2016. Assessing hydrodynamic space use of brown trout, *Salmo trutta*, in a complex flow environment: a return to first principles. J. Exp. Biol. 219 (21), 3480–3491. https://doi.org/10.1242/jeb.134775.

Lagarrigue, T., Céréghino, R., Lim, P., Reyes-Marchant, P., Chappaz, R., Lavandier, P., Belaud, A., 2002. Diel and seasonal variations in brown trout (salmo trutta) feeding patterns and relationship with invertebrate drift under natural and hydropeaking conditions in a mountain stream. Aquat. Living Resour. 15 (2), 129–137. https://doi.org/10.1016/S0990-7440(02)01152-X.

Larranaga, N., Valdimarsson, S., Linnansaari, T., Steingrímsson, S., 2018. Diel activity and foraging mode of juvenile arctic charr in fluctuating water flow. River Res. Appl. 34 (4), 348–356. https://doi.org/10.1002/rra.3256.

Liao, J.C., 2006. The role of the lateral line and vision on body kinematics and hydrodynamic preference of rainbow trout in turbulent flow. J. Exp. Biol. 209 (20), 4077–4090. https://doi.org/10.1242/jeb.02487.

Liao, J.C., 2007. A review of fish swimming mechanics and behaviour in altered flows. Philos. Trans. R. Soc. B 362 (1487), 1973–1993. https://doi.org/10.1098/rstb.2007.2082.

Liao, J.C., Beal, D.N., Lauder, G.V., Triantafyllou, M.S., 2003. The kármán gait: novel body kinematics of rainbow trout swimming in a vortex street. J. Exp. Biol. 206 (6), 1059–1073. https://doi.org/10.1242/jeb.00209.

Lin, K., Zhou, C., Xu, D., Guo, Q., Yang, X., Sun, C., 2018. Three-dimensional location of target fish by monocular infrared imaging sensor based on a l–z correlation model. Infrared Phys. Technol. 88, 106–113. https://doi.org/10.1016/j.infrared.2017.11.002.

Lobón-Cerviá, J., 1996. Response of a stream fish assemblage to a severe spate in northern Spain. Trans. Am. Fish. Soc. 125 (6), 913–919. https://doi.org/10.1577/1548-8659(1996)125<0913:ROASFA>2.3.CO;2.

Mameri, D., Hayes, D.S., Führer, S., Fauchery, E., Schmutz, S., Monserat, A., Hasler, T., Graf, D.R.M., Santos, J.M., Ferreira, M.T., Auer, S., 2023. Cold thermopeaking-induced drift of nase chondrostoma nasus larvae. Aquat. Sci. 85 (2), 56. https://doi.org/10.1007/s00027-023-00955-x.

Matte, Johnston, Patricia, Guay, Jean-Christophe, Belzile, Louis, Bergeron, Normand, 2024. Response of Juvenile Atlantic Salmon to Artificial Flow Downstream of an Hydroelectric Dam. in preparation. INRS, Québec.

Mchayk, A., Marttila, H., Klöve, B., Torabi Haghighi, A., 2024. Hydropeaking mitigation with re-regulation reservoirs [_eprint: https://onlinelibrary.wiley.com/doi/pdf/10.1002/rra.4290]. River Res. Appl. https://doi.org/10.1002/rra.4290. *n/a*.

Nagrodski, A., Raby, G.D., Hasler, C.T., Taylor, M.K., Cooke, S.J., 2012. Fish stranding in freshwater systems: sources, consequences, and mitigation. J. Environ. Manag. 103, 133–141. https://doi.org/10.1016/j.jenvman.2012.03.007.

Naudascher, R., Boes, R.M., Silva, L.G.M., Stocker, R., 2024. Fishtracking in Laboratory Setups in preparation.

Nislow, K.H., Folt, C., Seandel, M., 1998. Food and foraging behavior in relation to microhabitat use and survival of age-0 atlantic salmon [Publisher: NRC Research Press]. Can. J. Fish. Aquat. Sci. 55 (1), 116–127. https://doi.org/10.1139/f97-222.

Pautsina, A., Císař, P., Štys, D., Terjesen, B.F., Espmark, Å.M.O., 2015. Infrared reflection system for indoor 3d tracking of fish. Aquac. Eng. 69, 7–17. https://doi.org/10.1016/j.aquaeng.2015.09.002.

Piccolo, J.J., Frank, B.M., Hayes, J.W., 2014. Food and space revisited: the role of drift-feeding theory in predicting the distribution, growth, and abundance of stream salmonids. Environ. Biol. Fish 97 (5), 475–488. https://doi.org/10.1007/s10641-014-0222-2.

Poff, N.L., Allan, J.D., Bain, M.B., Karr, J.R., Prestegaard, K.L., Richter, B.D., Sparks, R.E., Stromberg, J.C., 1997. The natural flow regime. BioScience 47 (11), 769–784. https://doi.org/10.2307/1313099.

Przybilla, A., Kunze, S., Rudert, A., Bleckmann, H., Brucker, C., 2010. Entraining in trout: a behavioural and hydrodynamic analysis. J. Exp. Biol. 213 (17), 2976–2986. https://doi.org/10.1242/jeb.041632.

Puffer, M., Berg, O.K., Huusko, A., Vehanen, T., Forseth, T., Einum, S., 2015. Seasonal effects of hydropeaking on growth, energetic and movement of juvenile Atlantic salmon (*Salmo Salar*): effects of hydropeaking on juvenile Atlantic salmon. River Res. Appl. 31 (9), 1101–1108. https://doi.org/10.1002/rra.2801.

Reindl, R., Neuner, J., Schletterer, M., 2023. Increased hydropower production and hydropeaking mitigation along the upper inn river (Tyrol, Austria) with a combination of buffer reservoirs, diversion hydropower plants and retention basins [_eprint: https://onlinelibrary.wiley.com/doi/pdf/10.1002/rra.4052]. River Res. Appl. 39 (3), 602–609. https://doi.org/10.1002/rra.4052.

Ribi, J.-M., Boillat, J.-L., Peter, A., Schleiss, A.J., 2014. Attractiveness of a lateral shelter in a channel as a refuge for juvenile brown trout during hydropeaking. Aquat. Sci. 76 (4), 527–541. https://doi.org/10.1007/s00027-014-0351-x.

Riley, W.D., Maxwell, D.L., Pawson, M.G., Ives, M.J., 2009. The effects of low summer flow on wild salmon (salmo salar), trout (salmo trutta) and grayling (thymallus thymallus) in a small stream. Freshw. Biol. 54 (12), 2581–2599. https://doi.org/10.1111/j.1365-2427.2009.02268.x.

Saltveit, S., Halleraker, J., Arnekleiv, J., Harby, A., 2001. Field experiments on stranding in juvenile Atlantic salmon (salmo salar) and brown trout (salmo trutta) during rapid flow decreases caused by hydropeaking. Regul. Rivers Res. Manag. 17 (4), 609–622. https://doi.org/10.1002/rrr.652.

Salvanes, A.G.V., Moberg, O., Ebbesson, L.O.E., Nilsen, T.O., Jensen, K.H., Braithwaite, V.A., 2013. Environmental enrichment promotes neural plasticity and cognitive ability in fish. Proc. Biol. Sci. 280 (1767), 20131331 https://doi.org/10.1098/rspb.2013.1331.

Schmutz, S., Bakken, T.H., Friedrich, T., Greimel, F., Harby, A., Jungwirth, M., Melcher, A., Unfer, G., Zeiringer, B., 2015. Response of fish communities to hydrological and morphological alterations in hydropeaking rivers of Austria. River Res. Appl. 31 (8), 919–930. https://doi.org/10.1002/rra.2795.

Shen, Y., Diplas, P., 2010. Modeling unsteady flow characteristics of hydropeaking operations and their implications on fish habitat. J. Hydraul. Eng. 136 (12), 1053–1066. https://doi.org/10.1061/(ASCE)HY.1943-7900.0000112.

Sibeaux, A., Newport, C., Green, J.P., Karlsson, C., Engelmann, J., Burt De Perera, T., 2024. Taking a shortcut: what mechanisms do fish use? Communications Biology 7 (1), 578. https://doi.org/10.1038/s42003-024-06179-5.

Taguchi, M., Liao, J.C., 2011. Rainbow trout consume less oxygen in turbulence: the energetics of swimming behaviors at different speeds. J. Exp. Biol. 214 (9), 1428–1436. https://doi.org/10.1242/jeb.052027.

Tonolla. (2017). *Schwall-sunk – massnahmen. ein modul der vollzugshilfe renaturierung der gewässer.* Bundesamt für Umwelt, Bern. https://www.bafu.admin.ch/bafu/en/home/topics/water/water–publications/publications-water/schwall- sunk- massnahmen.html.

Tuhtan, J.A., Noack, M., Wieprecht, S., 2012. Estimating stranding risk due to hydropeaking for juvenile european grayling considering river morphology. KSCE J. Civ. Eng. 16 (2), 197–206. https://doi.org/10.1007/s12205-012-0002-5.

Vanzo, D., Bejarano, M.D., Boavida, I., Carolli, M., Venus, T.E., Casas-Mulet, R., 2023. Innovations in hydropeaking research. River Res. Appl. 39 (3), 277–282. https://doi.org/10.1002/rra.4118.

Walter, T., Couzin, I.D., 2021. TRex, a fast multi-animal tracking system with markerless identification, and 2d estimation of posture and visual fields. eLife 10, e64000. https://doi.org/10.7554/eLife.64000.

Webb, P.W., 1994, September 15. The biology of fish swimming. In: Maddock, L., Bone, Q., Rayner, J.M.V. (Eds.), The Mechanics and Physiology of Animal Swimming, 1st ed. Cambridge University Press, pp. 45–62. https://doi.org/10.1017/CBO9780511983641.005.

Würsig, B., 2009, January 1. Bow-riding. In: Perrin, W.F., Würsig, B., Thewissen, J.G.M. (Eds.), Encyclopedia of Marine Mammals, second edition. Academic Press, pp. 133–134. https://doi.org/10.1016/B978-0-12-373553-9.00037-7.

Young, P.S., Cech, J.J., Thompson, L.C., 2011. Hydropower-related pulsed-flowimpacts on stream fishes: a brief review, conceptual model, knowledge gaps, and research needs. Rev. Fish Biol. Fish. 21 (4), 713–731. https://doi.org/10.1007/s11160-011-9211-0.

Zitek, A., Schmutz, S., Unfer, G., Ploner, A., 2004. Fish drift in a danube sidearm-system: I. site-, inter- and intraspecific patterns [_eprint: https://onlinelibrary.wiley.com/doi/pdf/10.1111/j.0022-1112.2004.00533.x]. J. Fish Biol. 65 (5), 1319–1338. https://doi.org/10.1111/j.0022-1112.2004.00533.x.